Electric Propulsion Torsional Thrust Balance with Wireless Microwave Power Transfer

Conference Paper · March 2021

CITATIONS
3

READS
561

8 authors, including:

Kyaw Swar
Added Value Solutions UK
7 PUBLICATIONS **39** CITATIONS
SEE PROFILE

Emmanuelle Rosati Azevedo
Imperial College London
21 PUBLICATIONS **125** CITATIONS
SEE PROFILE

Alberto Garbayo
URA Thrusters
19 PUBLICATIONS **98** CITATIONS
SEE PROFILE

ELECTRIC PROPULSION TORSIONAL THRUST BALANCE WITH WIRELESS MICROWAVE POWER TRANSFER

17 – 18 – 19 MARCH 2021

K. Swar [(1)], D. Staab [(1)], E. Rosati Azevedo [(1)], A. Garbayo [(1)], S. Masillo [(2)], J. Stubbing [(2)], A. Lucca Fabris [(2)], R. Moloney [(2)]

[(1)] Added Value Solutions UK Ltd., Rutherford Appleton Laboratory, Harwell, United Kingdom, Email: kswar@a-v-s.uk
[(2)] University of Surrey, Surrey, United Kingdom

KEYWORDS: electric propulsion, microwave, thrust balance, measurement, diagnostics, xenon, torsional, load cell, flex pivot

ABSTRACT:

AVS UK has designed, built, and tested a torsional thrust balance system with wireless radio frequency (RF) power transfer at the electric propulsion lab at the Surrey Space Centre (SSC). Following integration, and characterisation tests such as wireless power transfer efficiency, and thermal drift, it was used for the main test campaign of AQUAJET, an ECR thruster development model built by AVS UK. The thrust balance is tested through a measurement range from a few μN to several mN. This paper covers the detailed description of the balance design, calibration process, achieved calibration and measurement accuracy, and results of first AQUAJET thrust measurements.

1. INTRODUCTION

Added Value Solutions UK (AVS UK) is developing multiple propulsion devices such as AQUAJET, an electron-cyclotron resonance (ECR) thruster, XMET, Xenon microwave electro-thermal thruster, and XEPT, Xenon electric propulsion (EP) gridded ion thruster, and ICE, Iridium catalyst electrolysed thruster. Such devices produce thrust from <1mN to ~1N. Several institutional and commercial facilities have developed thrust balances that can measure from μN to hundreds of mN.

AVS UK has developed a torsional balance that can measure thrust from 0.1mN to 10mN with an achieved accuracy better than 10% and drift better than 1μN/min under thermal load in steady state. Significant challenges associated with measuring low thrusts at high resolutions arise from thermal expansion of structural materials and electrical harnesses, pressurisation and hysteresis of propellant feedlines, and electro-magnetic interferences on measurement instruments from the operation of thrusters. The vacuum environment introduces further challenges by reducing heat dissipation due to the lack of convective cooling. The vacuum chamber may also distort, and the pumps add vibration noise into the thrust balance system. Our torsional thrust balance design is described in detail in [1].

The linear displacement resulting from rotation is measured at one end by an optical fibre displacement sensor (OFDS). Th displacement range of interest is in the single to hundreds of microns, therefore any cosine errors on thrust measurement due to the angular rotation is negligible. Since the flexure pivot acts as torsional spring and the beam displaces based on thrust, the system can be characterised simply by using Eq.1.

$$F = k\Delta x \qquad Eq.1$$

where F is force, k is the calibration spring constant or overall stiffness of the system, and Δx is the displacement. This equation only holds true for equally distanced moment arm lengths. For asymmetric moment arms, a correction factor is required.

The commissioning, testing, and experimental campaign of the thrust balance and AQUAJET thruster was performed at the Surrey Space Centre's Daedalus facility consisting of a vacuum chamber measuring 1.5 m in diameter and 3 m in length, with a three-stage pumping system incorporating two cryogenic pumps in parallel with a turbomolecular pump. The chamber achieves a base pressure in the range of 10^{-7} Torr without mass flow injection.

2. PERFORMANCE METRICS

2.1. Sensitivity

For torsional thrust balances, the amount of deflection of the moment arm directly correlates to the resolution and precision of thrust measurements. Small forces can be optimally measured by maximising the moment arm length and minimising the spring constant. Sensor selection is critical due to a wide range of resolutions and ranges available.

2.2. Repeatability

Repeatability is determined by differences in measurements of the same absolute thrust over an extended amount of time. This is affected by drifts due to facility vibrations, thermal expansion, and stiffness contributions from cables and propellant feedlines. These stiffnesses can be reduced by using thin flexible cables and propellant lines.

2.3. Accuracy

A thrust balance must be able to measure thrust close to the true value of thrust. Therefore, a repeatable, set of loads tied to an absolute calibration standard must be applied during the calibration procedure. Ideally this should be performed in the same balance configuration and environment as the thruster test campaign itself e.g., under vacuum. To characterise accuracy, the thrust balance must be calibrated before and after a test campaign. The AVS thrust balance is calibrated in two ways. Primarily, a factory calibrated loadcell is pushed into the balance beam to measure the load-displacement relationship. This can be performed in either vacuum or ambient conditions. A secondary mass over pulley method is used to provide periodic coarse independent reference checks. This is achieved by attaching a string to the balance beam at the same moment arm length position as the loadcell. The string is routed over a bearing which acts as a pulley and a discrete number of calibrated masses are hung on the string to simulate a thrust force.

3. AVS THRUST BALANCE

The thrust stand consists of two main structures. The balance beam, where the thruster and counterweights are mounted, and the base plate, where the measurement instrumentation is

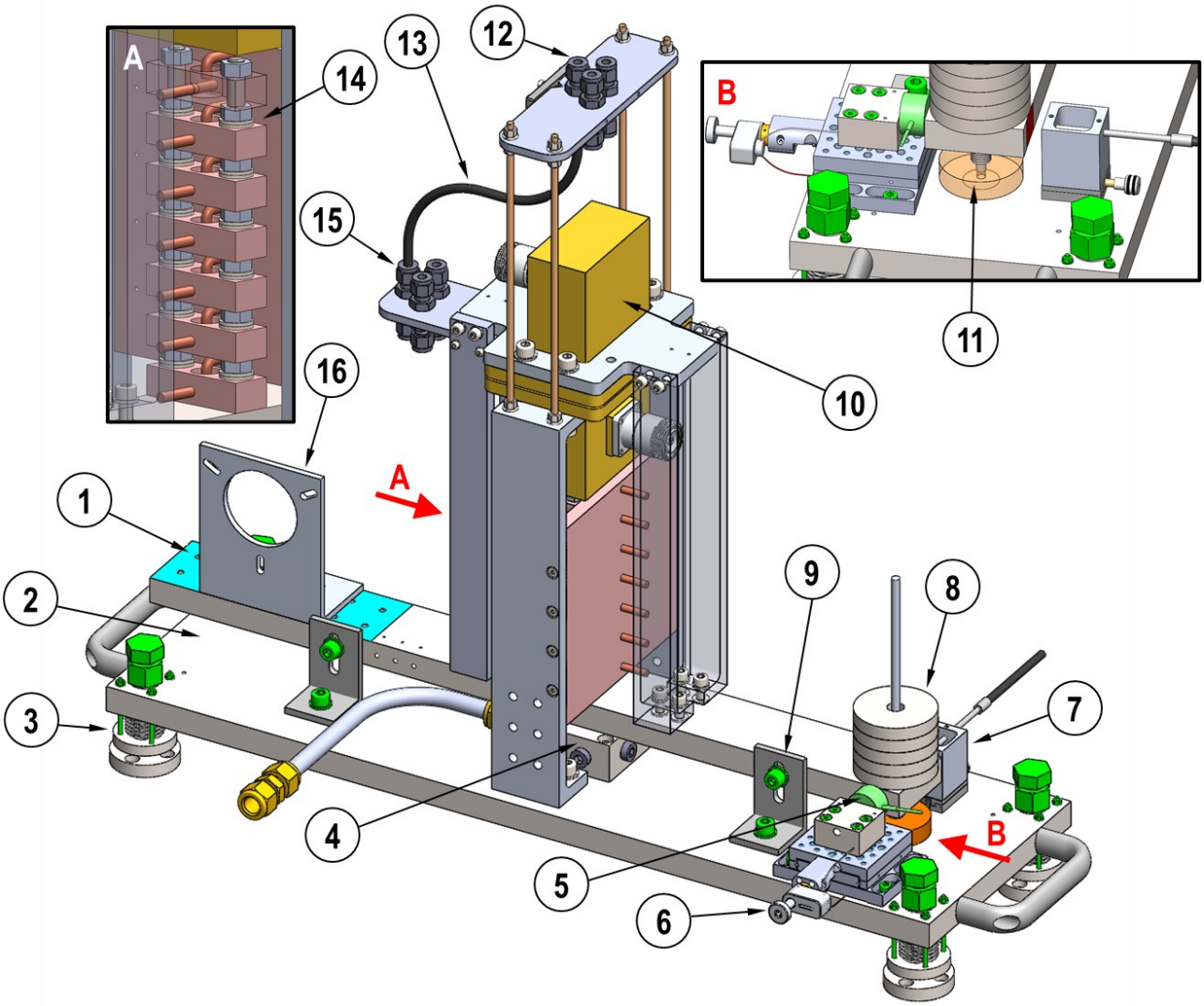

Figure 1. CAD drawing of the thrust balance design: 1. Balance beam (moving part). 2. Base plate (static part). 3. Vibration dampening feet. 4. Water-cooled flexure pivot hub. 5. Loadcell mounted on linear stage. 6. Piezomotor to actuate linear stage. 7. Optical Fibre Displacement Sensor. 8. Counterweights. 9. Locking brackets for assembly and safety. 10. Waveguides, 11. Copper disk and neodymium magnet for eddy brake 12. Static part propellant line bulkheads 13. Propellant line (single line pictured, capacity of up to 3 lines). 14. Liquid metal electrical connectors 15. Moving part propellant line bulkheads. 16. Thruster Interface Plate for AQUAJET.

mounted. Both structures are made from titanium to reduce thermal expansion effects and heat transfer from the thruster to the flexure pivot. A calibration loadcell (F329, Novatech) is mounted on a motorised linear stage to perform the calibration procedure and the OFDS is mounted in line with the loadcell travel on the opposite side of the base plate to view the displacement of the balance beam. The processing electronics for the loadcell and OFDS are placed outside the vacuum chamber away from the interference of any operating thrusters. An Eddy current damper is used to dampen the balance beam oscillations without introducing contact friction; a copper disc is mounted above neodymium disc magnets with a variable gap to control the level of dampening. The balance is electrically grounded to ensure that charge does not build up.

Non-magnetic materials are utilised where possible so that phantom forces are not measured due to interaction with the magnetic fields present in the thrusters. A novel contactless RF coupling waveguide is used to transmit RF power to the thruster to reduce the stiffness contributions and thermal expansions from a coaxial cable. Seven DC electrical connections are routed through room temperature liquid metal pots with two separate copper pins per pot to ensure almost frictionless electrical contact between the moving and static parts of the thrust balance. These electrical connections are rated up to 120A each.

The base plate houses the pivot mount. The pivot mount is surrounded by a fluid path to provide water-cooling from an external water chiller, limiting thermal expansion of the flexure pivot. The base plate sits on four spring feet that provide simple mass dampening and allow tilt adjustability of the entire balance system. A spirit level with a sensitivity of 0.3mm/m is used to ensure tilt is aligned with local gravity vector as misalignments can introduce zero thrust offsets and instabilities to the system. [2]

Since our description of the balance in [1], the setup has been modified slightly to include a wiring and propellant line cascade to accommodate thermocouple wires and flexible Tygon tubing close to the pivot axis. These lines flow down from the top of the balance where they are fixed to the static part of the balance. Their length is maximised as much as possible to ensure minimum stiffness and they are fixed on the moving part of the balance to ensure repeatable behaviour.

3.1. WAVEGUIDE COUPLING

AQUAJET requires 30-500 Watts of microwave power to operate within the 2.3-2.5GHz range. The standard method would be to use a thick, high stiffness shielded coaxial cable. We opted to use two opposing WR340 waveguide to coaxial transitions (2.20GHz to 3.3GHz) with a contactless gap of 1mm to transmit microwave

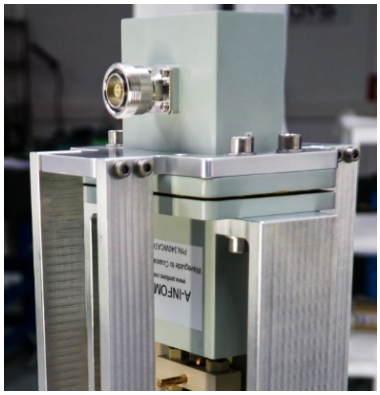

Figure 2. Waveguide transition arrangement for microwave power transfer. The top waveguide is fixed to the moving part and the bottom waveguide is fixed to the static part of the thrust balance.

power from the static to moving part of the thrust balance. This ensures that no parasitic torques are imparted onto the balance beam from the thermal expansion of the coaxial cables and no extra stiffness is added to the system.

PEEK washers are used for mounting the waveguides to the rest of the thrust balance structure. Combined with the contactless gap, this ensures electrical isolation and blocks transmission of any DC current through the microwave line. This is vital for the operation of microwave powered cathodeless ambipolar thrusters such as AQUAJET. [3] [4]

The 1mm gap is far smaller than the microwave wavelength at 2.45GHz, the nominal operation frequency of AQUAJET, therefore small transmission losses can be expected. A COMSOL model was used to quantify the microwave transmission losses as a function of gap distance as well as rotational angle using the exact waveguide interface geometry and performing an S-parameter calculation. The maximum rotation angle was set at 0.1 degrees, which is representative of the highest deflection of the thrust balance beam. Lateral in-plane misalignments between waveguides of up to 3mm were also modelled. All simulations resulted in less than 2% transmission loss. [1]

As the wireless gap features localised high electric field strengths, we assessed the potential for electric breakdown to occur in this region within representative vacuum conditions. Such a breakdown could cause localised plasma production at high input power levels with unknown effects on the balance's repeatability, and in the worst-case component failure. During thruster operation, the vacuum chamber background pressure will always be $<10^{-3}$ Torr, which is the threshold for multipactor microwave breakdown effects. In this regime, breakdown is pressure independent and it can occur if a critical voltage between small gaps is exceeded. According to ECSS-E-20-01A methodology and multipactor breakdown calculation, the breakdown voltage is 100V exactly at 2.45GHz for 1mm gap between bare aluminium surfaces (as for our waveguides).

[5] Using the same Multiphysics model as for the transmission loss calculation, the maximum voltage calculated is 49V at 500W of input power which gives us a factor of safety of 2 at the maximum design power of our thruster.

After manufacturing and assembly, the gap extended to 1.6mm. We verified experimentally the transmission losses from the gap and as a whole microwave transmission system compared to a line without waveguides in ambient conditions.

Table 1. Wireless line components for testing transmission loss across waveguide gap

Item	Manufacturer and Part No.	Insertion loss/dB
Type N (M) to 7/16 (F) adaptor	Huber & Suhner 716-4757	0.05
7/16 (M) to 7/16 (M) cable	7/16 (male) – 7/16 (male) SUCOFEED-1/2-HF coaxial cable, Length:1m	0.21
7/16 feedthrough	Allectra 242-7_16-K50	0.1
7/16 (M) to 7/16 (M) cable	Huber & Suhner 126-3133	Estimated 1.22 @ 2.45 GHz
(2x) Waveguides	A-info 340WCA7/16	0.14 + 0.13 (As tested directly by A-info)
Predicted wireless leakage loss	N/A	<0.09
7/16 (M) to Type N (M) cable	Huber & Suhner 126-3135	Estimated 1.22 dB @ 2.45 GHz
Total		3.14

Tab.1 shows the list of coaxial coupling components used in the test setup. The total line losses were compared to a) the same setup but with the gap zeroed by resting the two waveguides atop each other and b) to a setup where a female-to-female 7/16 connector replaced the waveguides. A microwave power generator (KU SG 2.45-250A, Kuhne) and a 50 ohm dummy load (6560.41.AA, Huber & Suhner) were used to simulate the power source and thruster power sink. An inline power meter (MA24105A, Anritsu) was used to monitor the forward power just before the dummy load.

Fig. 3 shows the test results where the total wireless transmission losses are around 5-7% including the losses from the waveguide gap in addition to baseline insertion losses of connector components. At 2.45 GHz, the inferred wireless "gap only" loss is as predicted by modelling at the ~2% level. The losses increase up to ~4% at 2.5 GHz though this frequency was not modelled. Overall, these results match our expectations of a suitably low-loss system, validating the wireless waveguide coupling system.

4. THERMAL DRIFT

During long duration operation of EP thrusters, they can dissipate significant waste heat to their surroundings. Due to the vacuum environment, heat can be transferred only through radiation and conduction. Therefore, the thrust balance must be designed to ensure the thermal loads do not significantly distort the flexural pivot, expand any structural materials or cabling driving variable stiffnesses or phantom thrust offsets.

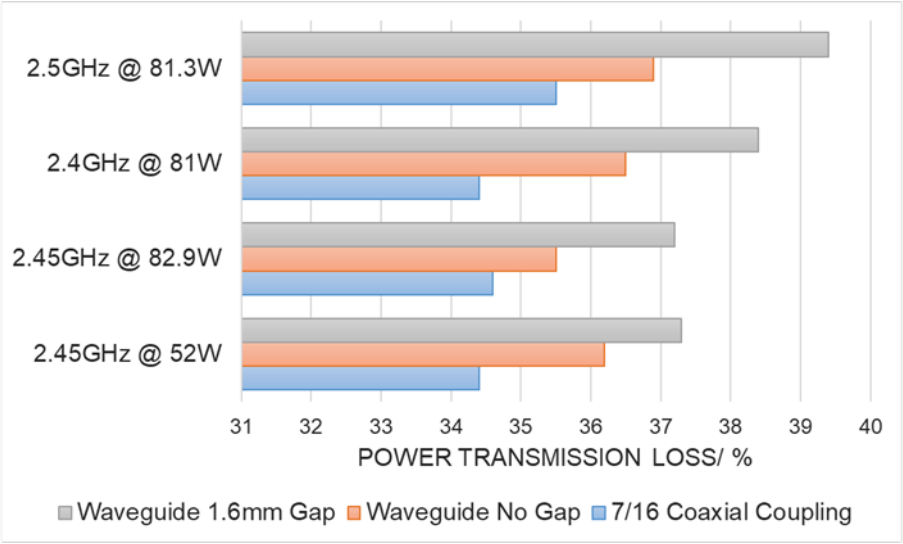

Figure 3. Microwave transmission line losses as verified experimentally in ambient conditions using a power generator and a dummy load to represent the thruster.

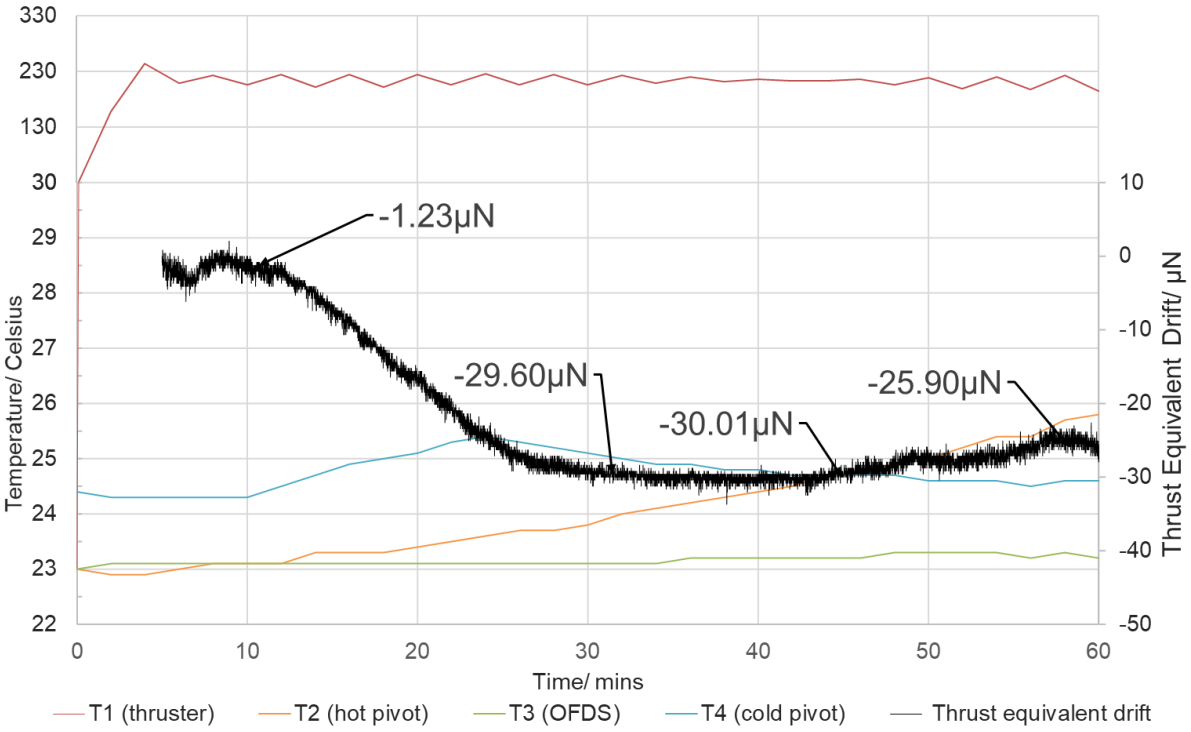

Figure 4. Thermal drift performance of the thrust balance over 1 hour in 1mbar rough vacuum condition. T1 represents the thruster interface plate temperature with heater tape wrapped around it to simulate a thruster heat load.

The AVS thrust balance is equipped with a water-cooling hub around the flex pivot. The hub contains an internal U-shaped channel that wraps around the pivot shaft. This hub is connected to an external room temperature water chiller. Additionally, titanium is used in critical structural parts to ensure thermal expansion and conductivity are minimised. The AQUAJET mounting interface also includes thermal insulation washers (DJB washers, Misumi) for thermal and electrical isolation.

To characterise thermal drift effects of the thrust balance at an extreme worst case, a fibreglass heater tape with 13.1W/in^2 was wrapped around the thruster interface plate to simulate a thruster heat load. Thermocouples are placed on the interface plate, OFDS target area on the balance beam, flex pivot set screws on the balance beam and water-cooled block. The tests were performed in rough vacuum conditions at around 1 mbar. The test was carried out by recording the zero-load deflection drift of the thrust balance beam while the heater was switched on and set at 200C with a simple PID controller.

Fig. 4 shows the pivots rise in temperature by only 3C with water-cooling activated and the hot end of the flex pivot has not reached steady state after 60 minutes. Extended data (not pictured) show that the hot pivot reaches a delta T of 5 degrees at 100 minutes. Note that the cold pivot temperature starts from a higher temperature than ambient due to the water chiller position in the lab directly next to a warm air vent. Due to thermal isolation and the low conductivity of titanium, the OFDS reflective area does not rise in temperature significantly. The small temperature differential in the hot and cold ends of the pivot however seem to change the balance beam deflection while heating up. This may be due to the flexure pivots itself expanding or thermocouple wires and propellant lines expanding and imparting a small torque. The worst-case drift of ~0.28µm/min and calibration constant of 6.66mN/mm is used to estimate a thrust-equivalent drift of 1.88µN/min in the transient period of approximately 30 minutes. After 30 minutes, the thrust equivalent drift falls below 1µN/min.

4.1. CALIBRATION AND ANALYSIS

To translate deflection of the balance beam into known forces, calibration is required to obtain the stiffness of the system. To characterise this relationship between deflection and thrust, a loadcell mounted on a motorised linear stage is pushed against the balance beam. The loadcell can measure forces up to 100mN and it is paired with a digital signal conditioner (DSCUSB, Novatech). The loadcell has a flat live boss with M2 thread to interface with load. A dial gauge type ball tip was installed on the live boss to provide better mechanical contact with the balance beam. Kapton tape was applied on the balance beam contact area to provide a smoother surface where the ball tip touches the beam.

Multiple calibrations were performed in both ambient, and vacuum conditions. A typical calibration sequence is shown in Fig. 5 and the linear fit to the average of 6 calibration sequences is shown in Fig. 7. We typically perform 3

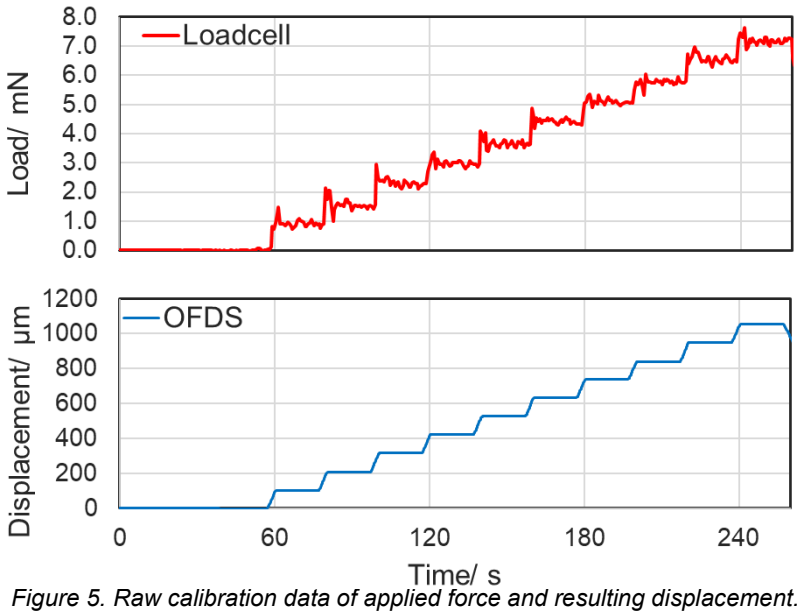

Figure 5. Raw calibration data of applied force and resulting displacement.

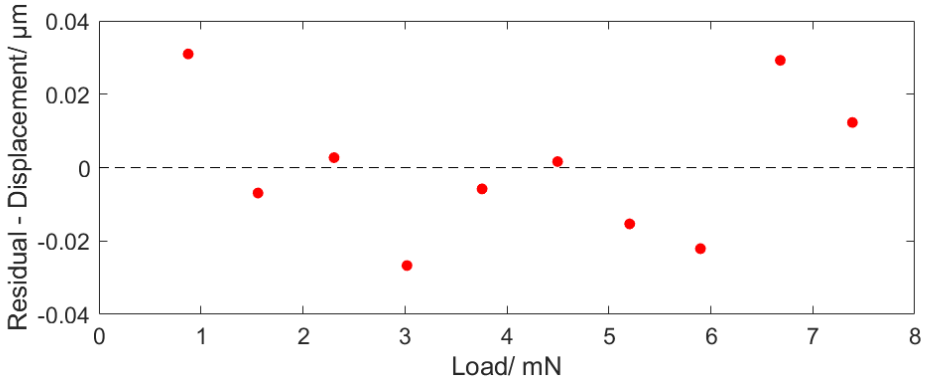

Figure 6. Residuals of the observed force vs estimated line of best fit.

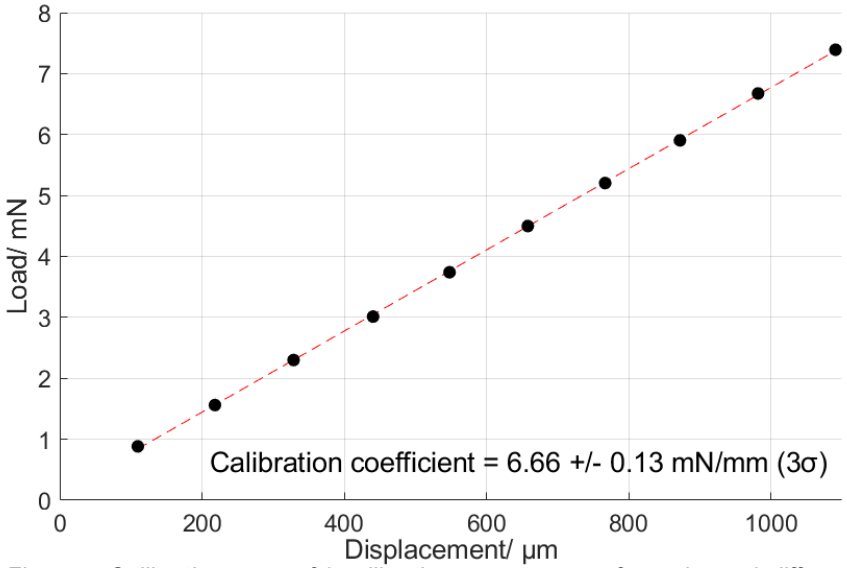

Figure 7. Calibration curve of 6 calibration sequences performed over 2 different sessions.

calibrations per thruster configuration or any other setup change to the balance-thruster system. The OFDS data are sampled at 5Hz and loadcell data are sampled at 2Hz. A calibration sequence takes about 5 minutes per run. During a calibration sequence, the loadcell is pushed into the thrust balance beam for 10 incremental displacements with 20 second dwell time at each step up to a maximum load matched to the thrust campaign range. This is done automatically by a python script controlling the linear stage piezomotor, minimising operator input and ensuring repeatability. The stiffness of the balance is 6.66mN/mm with 1.95% best-fit uncertainty at the

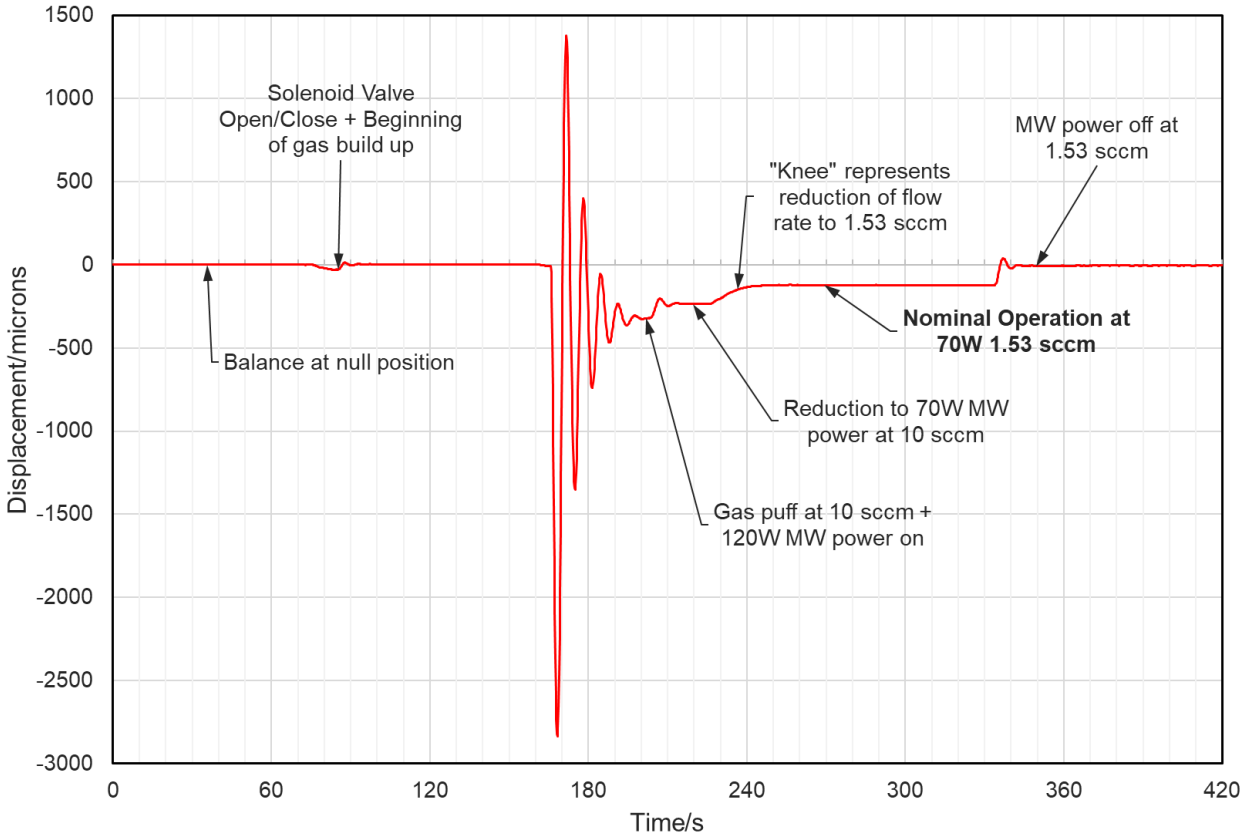

Figure 8. Displacement measurement of AQUAJET operating at 70W microwave power, nominal flowrate of 1.53 sccm of Xenon. The displacement step from nominal operation to MW power off represents 0.78mN of thrust.

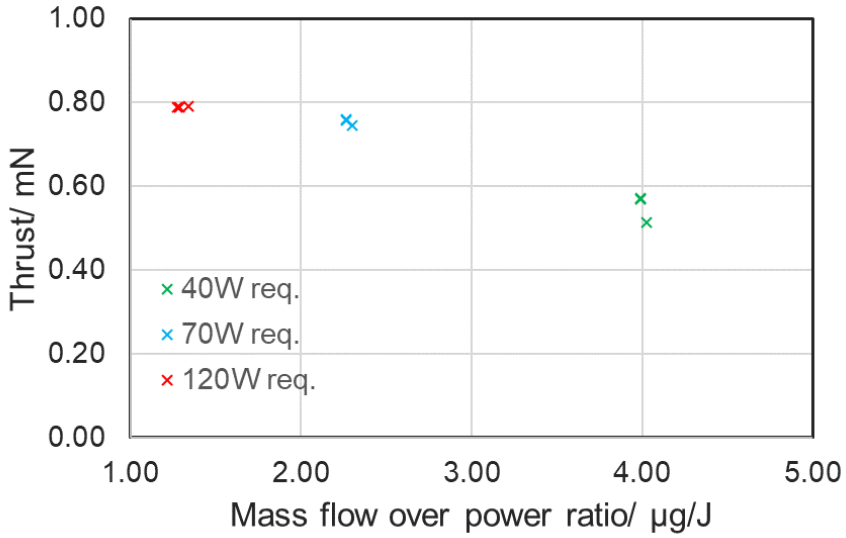

Figure 9. Thrust as a function of mass flow over power ratio. Each power level was tested 3 times to characterise repeatibility of the thruster-balance system.

3-sigma confidence level. We also plotted the residuals to assess linearity of the stiffness as shown in Fig 7. The observed values should be normally distributed around zero. There is a slight pattern seen in the residuals which is indicative of non-linearity. The residuals from a quadratic fit did follow a normal distribution. The largest deviation of the quadratic fit from the linear fit is only 0.1% relative to the full-scale range. Therefore, the linear fit is justified for use. These calibrations are performed after the cryo-pumps have been turned off but still in high vacuum as the pumps introduced high vertical vibrations on the thrust balance transferring onto the relatively fragile tip of the loadcell.

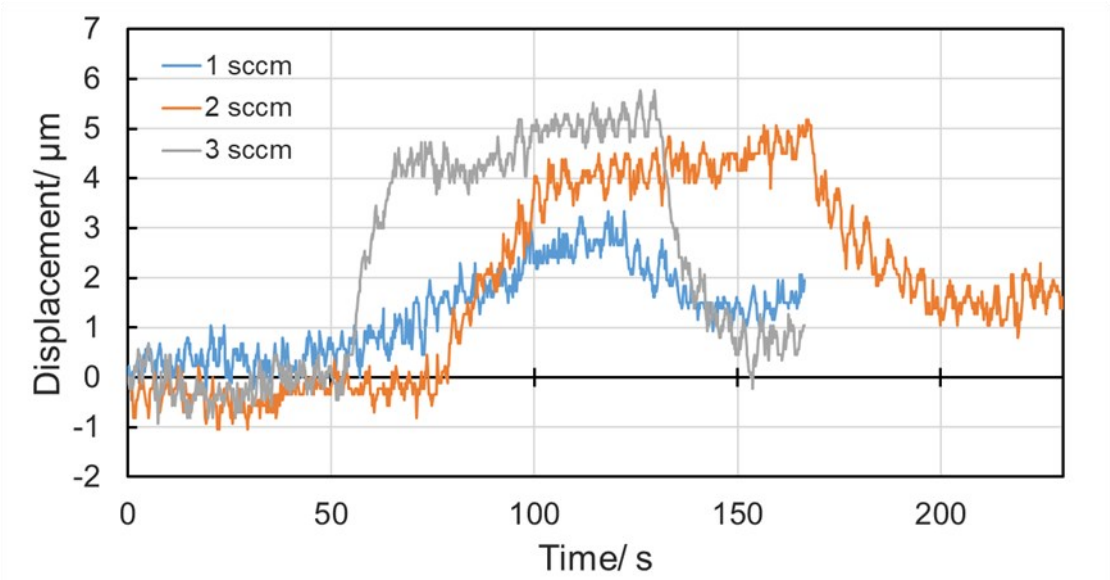

Figure 10. Displacement measurement of thrust balance with AQUAJET cold flow. The maximum displacement of 5µm corresponds to a thrust of 33µN.

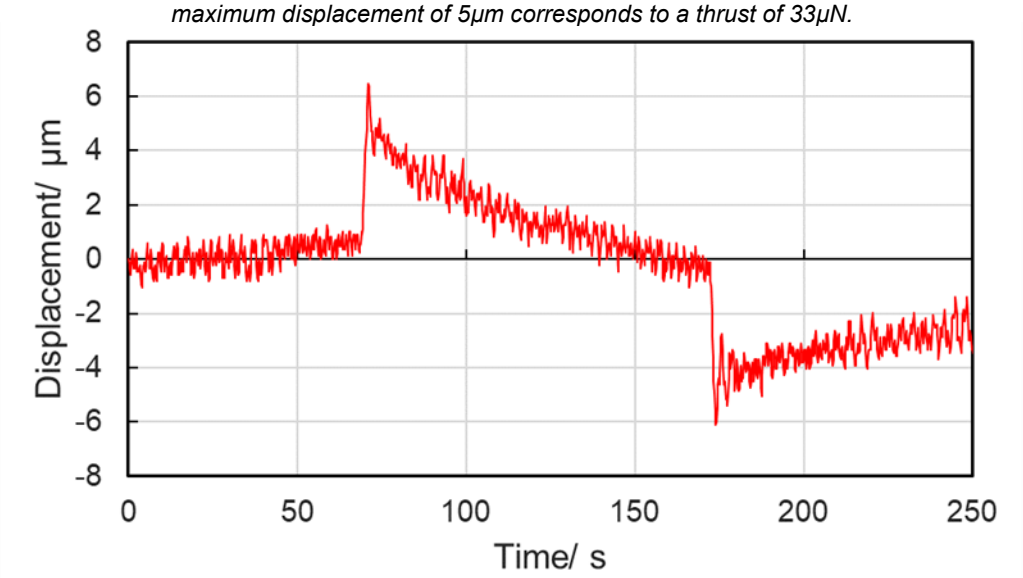

Figure 11. Displacement due to microwave line activation at 120W without gas flow. The maximum displacement step of 5µm corresponds to a thrust of 33µN.

A reference set of calibration was also carried out using the calibrated masses over a pulley to validate the loadcell calibration method. This method yielded a calibration constant 7% stiffer than the loadcell method and the discrepancy can be explained by the manual nature of the test method resulting in less repeatability as well as friction contribution from the pulley bearing.

5. THRUSTER TESTING AND REPEATIBILITY

In this section, we present thrust measurements of a development model of our ECR thruster, AQUAJET. Further details on AQUAJET design and performance can be found in SPC2020_00158 [7]. In Fig. 9. the output of the displacement sensor during a firing of the AQUAJET is shown. To ignite AQUAJET, a gas puff and microwave power higher than the nominal set-points are required. To build up to a gas puff, a solenoid valve mounted on the balance beam closes the propellant line while a gas flow of 10 sccm flows up to the valve. This solenoid shut-off vibration is first detected at around 80 s. At around 175 s, the build-up of gas is released while the microwave power is turned on simultaneously at 120W. The resulting thrust level from plasma ignition settles at around 200 s and the microwave power is reduced to the nominal operating power of 70W which settles at around 210 s. Then gas flow is reduced to the desired set-point of 1.53 sccm represented by the slowly reducing displacement (“knee” section) on the figure. The stable period from 250 to 330 s represents steady state AQUAJET operation at 70W and 1.53 sccm. At 340 s, the microwave power is shut off with gas flow still running. This displacement jump is finally used as the thrust step for the performance measurement. The net displacement is 115µm. Given that the calibration constant is 6.66mN/mm, this equals to a thrust of 0.77±0.015mN.

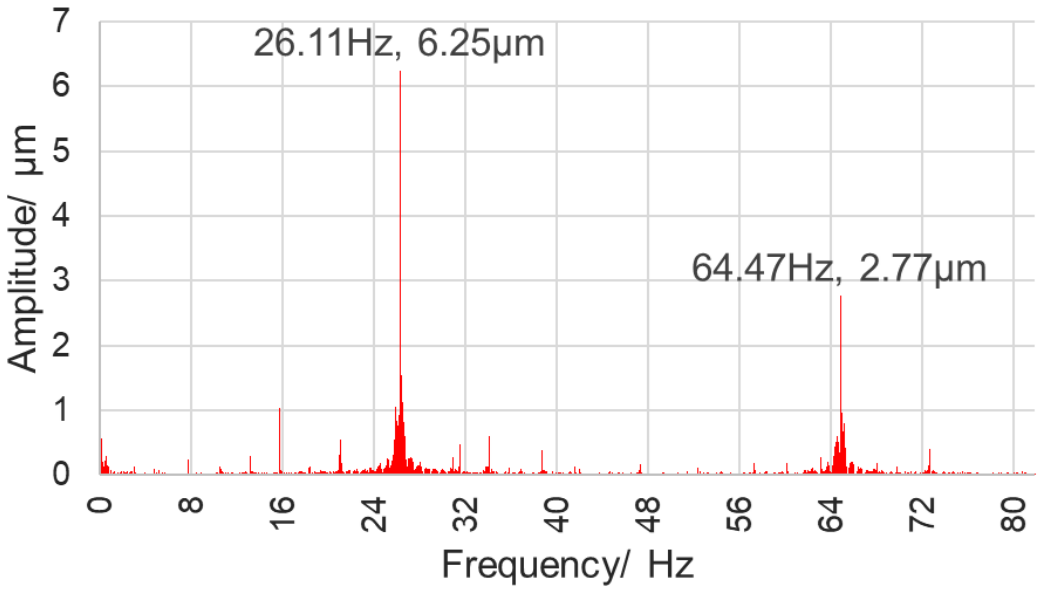

Figure 12. Fast Fourier Transform of OFDS measurement with all vacuum pumps and flexure pivot water-cooling switched on. Note that this vibration amplitude is the worst case.

Fig. 10 shows repeated thrust performance data collected in the same way, recorded as a function of mass flow rate over power ratio. There are 3 measurements per flowrate/power ratio regime with one measurement recorded on the first day and the rest recorded on a subsequent day to assess repeatability of the thrust balance. The worst-case repeatability of ~7% was observed for the 40W power level dataset, with 1.3% repeatability at the other power levels. AQUAJET performance measurements are not an ideal method to verify thrust balance repeatability as other factors such as vacuum level, power absorbed, plasma instabilities and flowrates can affect true thrust level repeatability significantly. A better method would be to use a simple and well characterised thruster as a reference such as a cold gas thruster [6], which is left for future work.

5.1. NON-THERMAL DRIFT AND PHANTOM THRUST CHARACTERISATION

To measure accurate thrust at mN and sub-mN levels, various effects must be considered such as propellant line drifts, and phantom thrust contributions from facility and supporting equipment.

Two tests were carried out to characterise these effects. The first test consisted of flowing propellant through the thruster at increasing flowrates without plasma ignition to determine the displacement response. Fig. 11 shows this effect for 3 flowrates. The worst-case effect at 3 sccm corresponds to ~33μN which is insignificant as thrust measurements with plasma ignition at that flow rate and corresponding power set point of 70W produces 1.12mN of thrust leading to less than 3% influence on the final thrust measurement.

The second test characterised displacement behaviour while only microwave power is transmitted to the thruster without propellant flow. The displacement of the balance was measured with the microwave generator at power set points corresponding to the AQUAJET operational parameters (40, 70, 120W). Displacement was only seen at 120W. Fig. 12 shows this effect at 120W microwave power corresponding to a maximum phantom thrust of ~33μN and associated drift. This effect is unexpected as the stiffness and any mechanical property change of the microwave line should not affect the balance beam position due to the mechanically decoupled wireless waveguide transmission. The behaviour was also observed only on three out of four tests. However, the amplitude of the effect is again insignificant compared to the 0.2 - 4 mN thrust range of interest for the AQUAJET campaign.

6. VIBRATION CHARACTERISATION

To measure the severity of facility vibrations on the thrust balance, high frequency OFDS readings were analysed in the frequency domain. The sampling frequency was increased to 163Hz from the nominal rate of 5Hz to capture higher order frequencies associated with vacuum pumps. This allowed us to observe horizontal vibrations of the balance beam due to vacuum pump induced mechanical vibrations in the vacuum chamber facility. The amplitude of these vibrations was then measured in terms of beam displacement.

A series of measurements were carried out by switching on vacuum pumps in a systematic sequence as well as the water pump for the flexure pivot water cooling loop. Measurements were taken at ambient with all pumps off as control. Roughing pumps, turbomolecular pumps, cryopump 1, cryopump 2, and cryo-panels were

each turned on in that sequence with measurements taken after each device activation.

Activation of the water-cooling loop for flexure pivots did not introduce any detectable vibrations. We observed worst case vibration amplitudes when all pumps were activated with 6.25μm at 26.11Hz (considering 6.66mN/mm calibration constant) as shown in Fig. 12. This translates to around 42μN of thrust equivalent noise. Other significant sources of noise occur at 64.5Hz with amplitudes around 3μm or less correlating to 20μN of thrust equivalent noise. This vibration at 64.5Hz was detected from roughing pump activation while the 26.1Hz vibration can be identified as the cryopumps whereas no significant additional noise was detected from turbomolecular pumps activation nor cryo-panel activation.

When the OFDS is in its normal operation frequency of 5Hz, 0.5μm peak-to-peak noise over 5 mins duration is observed. Averaging over 3 seconds reduce this peak-to-peak value down to <0.2μm.

7. CONCLUSION

The AVS torsional balance was used successfully for measuring thrust of AQUAJET, an ECR thruster. The wireless RF power transmission waveguides were validated to be low-loss and were demonstrated successfully at 40, 70, and 120W forward power levels. Active thermal management through the water-cooled flexure pivot was validated, with measured thermal drift rates at <2μN/min during a worst-case test and below 1μN/min over a ~1-hour steady state. The stiffness value of the thrust balance was characterised with the AQUAJET test setup to be 6.66mN/mm with 2% uncertainty at 3 sigma confidence level and cross-compared with calibrated weights. Micronewton to millinewton level forces were measured successfully. Thrust measurement repeatability was verified to be within 7% at worst case using AQUAJET though a reference cold gas thruster should be used in the future as a better absolute thrust stability reference. AQUAJET cold flow and phantom thrust due to microwave power were confirmed to be low-level effects that did not bias thruster performance data significantly. Vibrational characteristics of the thrust balance within the facility was also measured with insignificant effects on thrust measurements when the vacuum chamber is in operation with all its pumps.

8. ACKNOWLEDGMENTS

The work described in this paper is funded by UK Space Agency's National Space Technology Programme in the framework of the "NSTP3-PF2-055" and "NSTP3-FS021" projects. AVS would also express their gratitude to the vacuum test facility staff at Surrey Space Centre for technical assistance during test integration and through test campaign.

9. REFERENCES

1. Swar, K., Staab, D., Garbayo, A., Shadbolt, L., Masillo, S., Fabris, A. L., ... & Moloney, R. "Design and testing of a μN mN torsional thrust balance with wireless microwave power transmission", IEPC-2019-413, Proceedings of the 36th International Electric Propulsion Conference, Vienna, Austria, 2019.
2. Ziemer, John K. "Performance measurements using a sub-micronewton resolution thrust stand.", IEPC-01-238, Proceedings of the 27th International Electric Propulsion Conference, California, United States, 2001.
3. Rosati Azevedo, E., et al., "Analytical Plasma Modelling and Design Upgrade for an ECR Thruster Operating on Water and Ammonia Propellants," IEPC-2019-638, Proceedings of the 36th International Electric Propulsion Conference, Vienna, Austria, 2019.
4. Moloney, R., Karadag, B., Lucca Fabris, A., Staab, D., Frey, A., Garbayo, A., Shadbolt, L., Rosati Azevedo, E., Faircloth, D., Lawrie, S., and Tarvainen, O., "Experimental Validation and Performance Measurements of an ECR Thruster Operating on Multiple Propellants", IEPC-2019-199, Proceedings of the 36th International Electric Propulsion Conference, Vienna, Austria, 2019.
5. Design, Multipaction, and E. C. S. S. Test. "Secretariat: ECSS-E-20-01A." ESA-ESTEC May 5 (2003)
6. Seifert, B., Reissner, A., Buldrini, N., Hörbe, T., Plesescu, F., Bulit, A., & Borras, E. B. "Verification of the FOTEC μN Thrust Balance at the ESA Propulsion Lab", IEPC-2015-258, Proceedings of the 34th International Electric Propulsion Conference and 6th Nano-satellite Symposium, Hyogo-Kobe, Japan, 2015.
7. Rosati Azevedo, E., Swar, K., Staab, D., Longhi, E., Garbayo, A., Karadag, B., Stubbing, J., Moloney, R., Lucca Fabris, A., le Toux, T., Tarvainen, O., Faircloth, D., "XJET: Design Upgrade and Preliminary Characterization for an Electrodeless ECR Thruster," in Proceedings of the 7th Space Propulsion Conference, Estoril, 2021.